

Phase-Averaging Wave Propagation Array Models

M. Folley

School of Planning, Architecture and Civil Engineering, Queen's University Belfast, Belfast,
Northern Ireland

11.1 INTRODUCTION AND FUNDAMENTAL PRINCIPLES

Before considering how wave energy converter (WEC) arrays can be represented and modelled in phase-averaged wave propagation models, it is necessary to understand how these models are formulated. Phase-averaged wave propagation models, also called spectral wave models, are used extensively to model how the sea-state varies both spatially and temporally. Indeed, these models are used extensively and successfully to estimate sea-states from a global scale, to a local inland sea (see, eg, [Swail et al., 2000](#); [Mattarolo et al., 2009](#); [Rusu and Guedes Soares, 2009](#)). For phase-averaged wave propagation models the sea-state is defined by the frequency and direction-dependent variation in the spectral variance density of the sea surface elevation, more commonly known as the wave spectrum. The spatial variation in the sea-state is defined using a structured or unstructured grid of points and the temporal variation in the sea-state is defined using a discrete series of time steps.

These wave propagation models are considered to be 'phase-averaged' because the spectrum contains only the magnitude of each spectral wave

component and does not contain any information about the phases of the spectral wave components. It is generally considered that the best estimates of the wave phases are that they are random and uncorrelated. Although in steep waves or in shallow water this is not correct, the significant advantages that a random wave phase assumption provides to the model typically more than compensates for the lack of correctness in these circumstances. These advantages are that linear wave theory can be used for the propagation of the spectral wave components and nonlinear random vibration theory can be used to estimate the source terms (see the following).

In a phase-averaged wave propagation model the sea-state is determined using a continuity equation, which describes the transport and conservation of the wave action density. The wave action density is equal to the wave energy density divided by the wave frequency and is used because this is conserved in the presence of background currents, whilst wave energy density is not ([Komen et al., 1994](#)). It may help to recognize that if there is no background current then this reduces to the conservation of wave energy density; however, wave action density is the more

fundamental conservation property so this is used in phase-averaged wave propagation models. Application of the continuity equation means that the rate of change of wave action density at a point is due to the sum of all net flows of wave action density into this point, plus any generation/dissipation of wave action density at the point.

In phase-averaged wave propagation models the wave action density is a function of five variables: the two spatial coordinates (x, y) , the wave frequency, the wave direction, and time. So, the continuity equation becomes

$$\frac{\partial N}{\partial t} + \nabla_x \cdot \left[(\vec{c}_g + \vec{U}) N \right] + \frac{\partial c_\sigma N}{\partial \sigma} + \frac{\partial c_\theta N}{\partial \theta} = \frac{S}{\sigma} \quad (11.1)$$

where N is the wave action density, c_g is the group velocity, U is the background current, and c_σ and c_θ are propagation velocities in spectral space where σ is the wave frequency, θ is the wave direction and S is the source strength that defines the generation/dissipation of wave energy.

Looking at Eq. (11.1) in more detail, the left-hand side of the equation models the transport of the wave action. Solving this requires the distribution of the wave action, together with values for background current, the wave group velocity and propagation velocities in spectral space. The group and propagation velocities are essentially calculated using linear wave theory, because it is computationally efficient and found to estimate the transport of the wave action reasonably well. In water of a constant depth and without currents the last two terms are zero, so, ignoring source terms, it can be seen that wave action simply propagates in the direction that the waves are travelling. If a variable depth is now considered then the waves will change direction due to refraction. Thus, the propagation velocity in directional space c_θ has a finite value and so the last term on the left-hand side of Eq. (11.1) needs to be included. Finally, adding a varying current means that the propagation velocity in both directional space and frequency space are both finite as currents can affect both the direction of wave propagation and the wave frequency. Consequently, all the

terms on the left-hand side of Eq. (11.1) are required where there is a background current.

The astute reader may realize that a phase-averaged representation of wave propagation is not able to directly model diffraction because it does not contain the necessary wave phase information. Not including diffraction in the model means that the sea-state behind bodies such as islands and headlands will not be modelled accurately. To overcome this shortcoming, a phase-decoupled refraction–diffraction approximation has been developed based on the mild-slope equation for refraction–diffraction, but omitting phase information (Holthuijsen et al., 2003). Although this approximation is not able to identify phase-dependent features such as partial standing waves and provides a relatively poor approximation close to singularities such as the tips of breakwaters, it has been found to provide a good approximation of the action density in the majority of relevant scenarios.

Returning to Eq. (11.1), the right-hand side of the equation represents the change in wave action density due to wave generation or wave dissipation processes. Virtually all current versions of phase-averaged wave propagation models include explicit representation of all the key processes and are called third-generation spectral wave models (first-generation models did not consider all the natural wave generation/dissipation processes and second-generation models used parameterizations). Examples of third-generation spectral wave models include SWAN, TOMAWAC, and Mike21SW. The natural processes included in these third-generation spectral wave models are:

- wind–wave growth
- bottom friction
- white-capping
- depth-induced wave breaking
- quadruplet wave–wave interactions
- triad wave–wave interactions

Details of how the change in action density is calculated for these processes is beyond the

scope of this book; for the interested reader further information can be found in [Komen et al. \(1994\)](#). However, in general the strength of the source term sensibly depends on the local conditions, such as the wave spectrum, wind speed, water depth, background current, etc. From extension it is reasonable that these parameters could also be used to calculate the change in wave action due to a WEC or WEC array. Thus, WECs can be represented in third-generation spectral wave models by the inclusion of additional source terms.

It should be recognized that a phase-averaged wave propagation model is not capable of determining how the WEC changes the wave action; this must be done by another model, but it can be used to estimate what impact the WEC or WEC array may have on surrounding wave conditions, or to calculate WEC array interactions. A particularly suitable model for the WEC is a spectral-domain model (see [Chapter 4](#)) because the model already contains the phase-averaged assumptions inherent in these wave models; however, data from any model (including a wave-tank model) could be used to estimate the impact of the WEC or WEC array on the wave field. Because another model is required to estimate the WEC response, in common with the modelling of WEC arrays using phase-resolved wave propagation models, it can be classified as a hybrid WEC array model.

The potential to represent WECs in third-generation spectral wave models has a number of significant advantages. A key advantage is that the core of the model already exists and so only an appropriate WEC source term needs to be developed. A related advantage is that third-generation spectral wave models are already used extensively in the modelling of wave transformation and so many users will be familiar with these models, which is likely to facilitate their application. Another key advantage is that very large WEC arrays can be modelled, including WEC arrays with hundreds of WECs and those distributed over seascapes of tens of

kilometres. Moreover, the WEC arrays can be modelled in an inhomogeneous wave field, which includes variations in the wave action density due to bathymetry and/or background currents, which could become more significant as the geographical size of the WEC array increases.

There are fundamentally two different approaches by which WECs can be included in a third-generation spectral wave model. The first method is to use a WEC representation that causes a change in the wave action density as it crosses a line defined by two or more geographical points; this is termed a supragrid model. The second method is to use a WEC representation that causes a change in the wave action density at a single grid point; this is termed a subgrid model. [Fig. 11.1](#) shows a comparison of the change in significant wave height for a constant water depth due to these two different approaches, taken from [Silverthorne and Folley \(2011\)](#). The differences between these two approaches are described in more detail in the following sections.

11.2 SUPRAGRID MODELS OF WEC ARRAYS

Many third-generation spectral wave models provide the potential to represent a breakwater defined by two or more geographical points. This has been used to represent a WEC array at the WaveHub site by [Millar et al. \(2007\)](#) in the SWAN model where it is possible to define an *OBSTACLE* with fixed transmission coefficients as defined in Eq. (11.2).

$$S_{\text{WEC}}(\sigma, \theta) = k_t \cdot E(\sigma, \theta) \quad (11.2)$$

where $S_{\text{WEC}}(\sigma, \theta)$ is the strength of the WEC source term, $E(\sigma, \theta)$ is the wave energy density and k_t is the transmission coefficient.

[Millar et al. \(2007\)](#) modelled the effect of the WEC array for a range of transmission coefficients to represent different types of array, from a widely spaced array to an array of densely

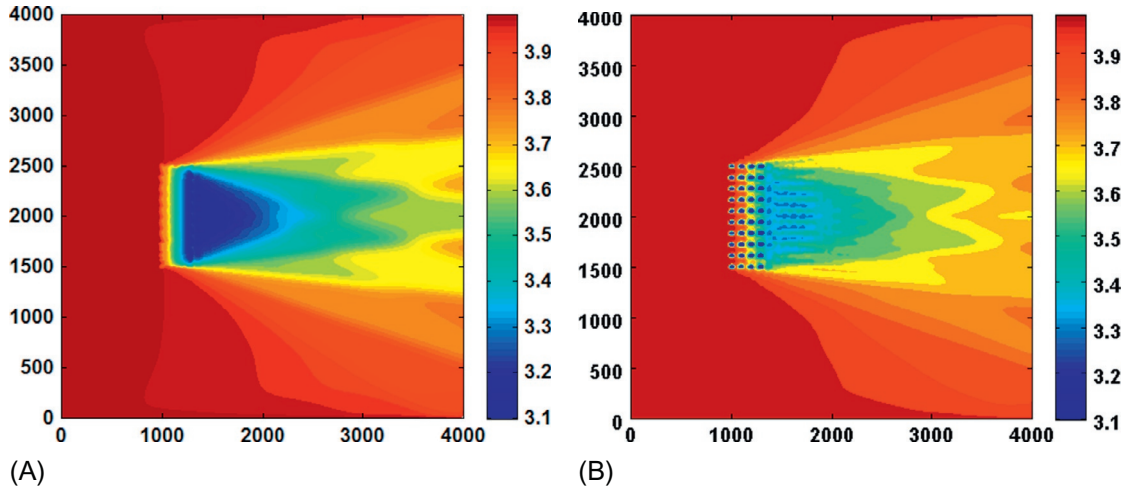


FIG. 11.1 Comparison of supragrid WEC array model (A) and subgrid WEC array model (B). From Silverthorne, K., Folley, M., 2011. A new numerical representation of wave energy converters in a spectral wave model. In: 9th European Wave and Tidal Energy Conference, Southampton, UK.

spaced, high efficiency WECs. A similar study was undertaken by Carballo and Iglesias (2013) for a WEC array deployed in Northwest Spain. However, in this case the values for the transmission and reflection coefficients used in the model were determined from wave-tank testing.

Without validation it is difficult to assess how accurate these models are; however, it would be reasonable to assume that for real WECs the coefficients will depend on the wave frequency, direction, and amplitude. Thus, an improvement to the simple use of the *OBSTACLE* source term in SWAN can be made by editing the FORTRAN code that defines the characteristics of the source term so that they are frequency and directionally dependent, as given by Eq. (11.3).

$$S_{\text{WEC}}(\sigma, \theta) = k_t(\sigma, \theta) \cdot E(\sigma, \theta) \quad (11.3)$$

This has been done by Smith et al. (2012) who compared the results with the model of Millar et al. (2007) and found that the impact of the wave farm was different between the models with constant and frequency-dependent transmission coefficients. Although the code

modification by Smith et al. (2012) also allows for the transmission coefficient to be directionally dependent, this functionality is not used. A more complete WEC source term would also include the wave amplitude in the calculation of the transmission coefficient, and/or include redistributed energy in a reflection coefficient. Although not included by Smith et al. (2012), this extension should be relatively simple to implement. What is likely to be more challenging is to determine what the transmission and reflection coefficient functions should be for a particular WEC or WEC array.

In principle, a supragrid model can be used either for a single WEC or for a WEC array. In either case the source term needs to represent the effect on the wave action density accurately. However, for it to be used for a single WEC the grid resolution needs to be significantly smaller than the WEC size, otherwise the WEC would be ‘missed’ if a grid point does not fall between the points defining the extent of the WEC. Moreover, even if a grid point does fall between the WEC extents the change in wave energy density may not be accurate because the integral of the

change in wave energy density may be very different from the actual change in wave energy due to the WEC. Consequently, a supragrid model is most suitable for large WECs such as Wave Dragon (Tedd and Kofoed, 2009) or a WEC array modelled as a single entity.

11.3 SUBGRID MODELS OF WEC ARRAYS

In subgrid models the effect of each WEC is concentrated at a single grid point. The use of subgrid models to represent WECs in a phase-averaged wave propagation model has only recently been developed where Silverthorne and Folley (2011) reported modelling an array of 40 WECs in four equal rows. In this case the open-source third-generation spectral wave model TOMAWAC (EDF, 2010) was modified to include a WEC source term that defined an absorption characteristic that could be frequency and directionally dependent. However, as with the supragrid model of Smith et al. (2012), the WEC modelled was not directionally dependent. The results from the subgrid model were compared to those using a supragrid model of the whole WEC array. It was noted that, although in the far field the effects on significant wave height were found to be similar, closer to the WECs the estimates of significant wave height differed as the supragrid could not capture the effect of the gaps between the WECs. Silverthorne and Folley (2011) also used the subgrid model to investigate how the power capture differed for each row in the WEC array, as well as the effect of removing a block of WECs in the array. However, although the results presented appear reasonable, they do not include any verification or validation, which would increase confidence in the accuracy of the model.

An important component of a subgrid model is that the wave energy extracted (or redistributed) for the waves by the WEC needs to be converted into a change in wave energy density so

that the strength of the WEC source term can be specified. It may be expected that this should be a relatively simple function, such as dividing the wave energy by the area adjacent to the grid point. However, defining the change in wave energy density as the change in wave energy divided by the adjacent area did not result in the correct change in wave energy in the TOMAWAC spectral wave model (Silverthorne and Folley, 2012). Silverthorne and Folley (2012) solved this by enforcing a fixed grid geometry surrounding each WEC and then calibrating the area using a separate simulation of a single WEC with only the WEC source term active and calculating the integral of wave energy passing through a closed loop surrounding the WEC. This integral equals the change in wave energy due to the WEC, which was achieved by defining an appropriate representative area that results in the required change in wave action density. Although successful, a more flexible solution is clearly desirable.

Another consideration when converting the change in wave energy into a change in wave energy density is ensuring that it is never greater than the incident wave energy density, as this would result in a negative wave energy density, which is nonsensical. This limit on the change in wave energy density effectively constrains the grid resolution so that there is a minimum cell size that will depend on the performance of the WEC being modelled. The maximum capture width of the WEC can be used as a guide to the maximum grid resolution, which suggests that for many WECs a minimum grid spacing of approximately 50 m should be acceptable, although this should always be explicitly checked.

Definition of a subgrid WEC source term requires consideration of how much wave energy is extracted from the incident waves, how much wave energy is absorbed and how the wave energy is redistributed. As previously noted, the derivation of the subgrid WEC source term strength requires the use of another WEC

model, but it can be included in whatever form is most convenient. Thus, the subgrid WEC source term could be defined by anything from a simple look-up table (as previously used for supragrid models) to a complex set of equations.

Although any suitable model may be used to derive the subgrid WEC source term strength, a particularly suitable model involves the use of Kochin functions for the definition of the redistributed wave energy (Babarit et al., 2013). Kochin functions define the far-field wave potential due to either diffraction or radiation as given by

$$\tilde{\phi}_k(r, \theta, \beta) = \sqrt{\frac{2}{\pi}} \frac{e^{i(kr - \pi/4)}}{\sqrt{kr}} H(\theta, \beta) \quad (11.4)$$

where $\tilde{\phi}_k$ is the far-field diffraction or radiation velocity potential, $H(\theta, \beta)$ is the Kochin function for a wave incident at the angle β , and kr is the nondimensional distance from the WEC. Solving the WEC response, which can be done in the WEC source term function, it is possible to calculate a net Kochin function by the complex sum of the diffraction and radiation Kochin functions, which has the same form as Eq. (11.4):

$$H(\theta, \beta) = A(\theta, \beta) \cdot H_{\text{diff}}(\theta, \beta) + R(\theta, \beta) \cdot H_{\text{rad}}(\theta, \beta) \quad (11.5)$$

where A is the incident wave amplitude and R is the complex WEC response amplitude.

By combining this far-field velocity potential with the velocity potential of the incident wave and then determining its asymptotic value as the

distance increases, it has been shown (Babarit et al., 2013) that the radial wave energy density J_r is given by

$$\begin{aligned} \bar{J}_r(r, \theta, \beta) = & J_i(\beta) \\ & \times \left(\cos(\theta - \beta) + \frac{2|H(\theta, \beta)|^2}{\pi kr} + \frac{4}{k} \Re(H(\theta, \beta)) \delta(\theta - \beta) \right) \end{aligned} \quad (11.6)$$

where $J_i(\beta)$ is the incident wave energy flux from the angle β and δ is the delta function, which is equal to zero except when $\theta = \beta$, where it is equal to 1.

The three terms on the right-hand side of Eq. (11.6) can be usefully associated with specific elements of the wave field. The first term is simply due to the incident wave, the second term is due to the diffracted/radiated waves and the third term is the reduction in the incident wave energy flux due to the wave energy absorbed and also redistributed. Thus, Kochin functions can be used to define the redistribution of the wave energy due to the combined effect of diffraction and radiation.

Fig. 11.2 shows the specific diffraction, specific radiation, and net Kochin functions for a pitching cylinder with a nondimensional radius of 0.5 that is optimally damped, but not tuned to the incident wave frequency. It can be seen that the diffracted waves are concentrated in the direction opposing the incident wave field, and that the radiated waves form a dipole pattern as would be expected for a pitching axisymmetric body. Importantly, the net Kochin

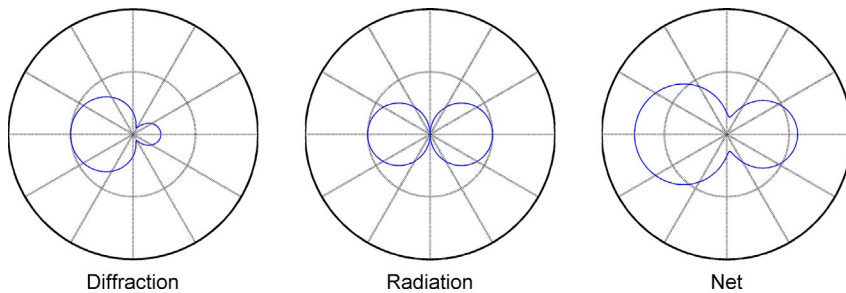


FIG. 11.2 Diffraction, radiation, and net Kochin functions for a pitching cylinder.

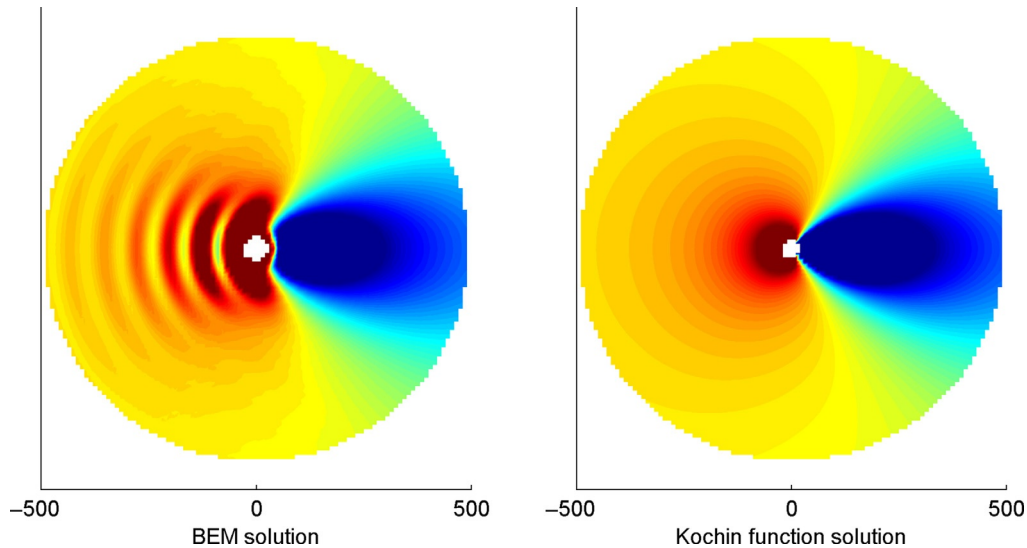


FIG. 11.3 Comparison of change to significant wave height due to a single WEC modelled using Kochin functions with the 'exact solution' based on a BEM.

function depends on the phase relationship between the incident wave and WEC response which produces the net wave pattern shown.

Fig. 11.3 shows the comparison of the estimated change in the surrounding significant wave height for a model that uses the 'exact' solution from a boundary element method (BEM) with the estimated change using Kochin functions for a directionally distributed Bretschneider sea-state. It can be seen that the two models estimate virtually identical changes to the wave fields. A small difference can be seen close to the WEC where a phase-dependent variation in the significant wave height is predicted by the BEM; however, this becomes negligible after 1–2 wavelengths away from the WEC.

11.4 LIMITATIONS

There are two fundamental limitations to the use of phase-averaged wave propagation models for the modelling of WEC arrays. The first fundamental limitation is that all of the

array interactions are modelled based on a phase-averaged assumption. This could be considered a significant limitation because the phase relationship between WECs in an array is known to have a significant influence on the magnitude of array interactions and net power capture. However, whilst at any single frequency phase-dependent interactions are known to be significant, their significance is significantly reduced for spectral sea-states (Folley and Whittaker, 2009). Related to this limitation is that the WEC near field is not accurately modelled, because not only is the near field phase-dependent, but also there is a nonpropagating (evanescent) wave field, which also cannot be modelled in a phase-averaged wave propagation model. The net consequence of these limitations is that the accuracy of WEC array interaction factors is reduced for close-packed arrays.

The second fundamental limitation is that this type of WEC array model requires another model (such as a spectral-domain model—see Chapter 4) to derive the characteristics of the WEC response. That is, a phase-averaged wave

propagation model can only be used to model the WEC array interactions; it cannot model the WEC itself. Consequently, the accuracy of the WEC array models depends not only on the accuracy of the phase-averaged wave propagation model, but also the accuracy of the model used to derive the WEC characteristics used in the model, together with the accuracy of the representation of these WEC characteristics in the phase-averaged wave propagation model.

A further limitation for supragrid models is that the grid resolution must be sufficiently fine to adequately represent the change in wave action density due to the WEC or WEC array. Conversely, a further limitation for subgrid models is that the grid resolution needs to be sufficiently coarse that the wave energy extracted for any single wave frequency and direction does not result in a reduction in the wave energy density that is greater than the incident wave energy density. These are unlikely to be significant limitations, except for small individual WECs for supragrid models and very closely spaced WEC arrays for subgrid models.

A final present limitation to the unrestrained use of phase-averaged wave models for the modelling of WEC arrays is that the techniques are relatively undeveloped and lack validation. This extends from the techniques for the development of representative WEC source terms to the assessment of the accuracy of the phase-averaged wave propagation. Thus, it would be premature to assess the full potential for this type of model because further developments may be possible and conversely it would be premature to rely extensively on this type of model because the model accuracy has not been fully determined.

11.5 SUMMARY

- Phase-averaged wave propagation models are based on conservation of action (energy) density; energy is added/removed through

source terms and propagated based on linear wave theory

- WECs can be represented as either supragrid elements or subgrid elements
- Phase-averaged wave propagation models are computationally efficient and capable of calculating the array interactions for very large, geographically distributed WEC arrays
- Phase-averaged wave propagation models are hybrid WEC array models because they require another model to calculate the response of single WECs that is then used in the WEC array model
- WECs may be represented using any structure, from a look-up table to a complex set of governing equations
- Kochin functions provide an efficient method to represent the directional redistribution of the wave energy due to a WEC in a subgrid array model
- Further development in the representation of WECs in phase-averaged wave propagation models is required

References

- Babarit, A., Folley, M., et al., 2013. On the modelling of WECs in wave models using far field coefficients. In: 10th European Wave and Tidal Energy Conference, Aalborg, Denmark. .
- Carballo, R., Iglesias, G., 2013. Wave farm impact based on realistic wave-WEC interaction. *Energy* 51, 216–229.
- EDF, 2010. TOMAWAC: Software for Sea State Modelling on Unstructured Grids Over Oceans and Coastal Seas. Release 6.0.
- Folley, M., Whittaker, T.J.T., 2009. The effect of sub-optimal control and the spectral wave climate on the performance of wave energy converter arrays. *Appl. Ocean Res.* 31 (4), 260–266.
- Holthuijsen, L.H., Herman, A., et al., 2003. Phase-decoupled refraction-diffraction for spectral wave models. *Coast. Eng.* 49 (4), 291–305.
- Komen, G.J., Cavaleri, L., et al., 1994. *Dynamics and Modelling of Ocean Waves*. Cambridge University Press, Cambridge.
- Mattarolo, G., Lafon, F., Benoit, M., 2009. Wave energy resource off the French coasts: the ANEMOC database

- applied to the energy yield evaluation of wave energy converters. In: 8th European Wave and Tidal Energy Conference, Uppsala, Sweden.
- Millar, D.L., Smith, H.C.M., et al., 2007. Modelling analysis of the sensitivity of shoreline change to a wave farm. *Ocean Eng.* 34 (5–6), 884–901.
- Rusu, E., Guedes Soares, C., 2009. Numerical modelling to estimate the spatial distribution of the wave energy in the Portuguese nearshore. *Renew. Energy* 34 (6), 1501–1516.
- Silverthorne, K., Folley, M., 2011. A new numerical representation of wave energy converters in a spectral wave model. In: 9th European Wave and Tidal Energy Conference, Southampton, UK.
- Silverthorne, K., Folley, M., 2012. Wave farm energy yield calculations using a modified spectral wave model. In: 19th Telemac and Mascaret User Club, Oxford, UK.
- Smith, H.C.M., Pearce, C., et al., 2012. Further analysis of change in nearshore wave climate due to an offshore wave farm: an enhanced case study for the Wave Hub site. *Renew. Energy* 40 (1), 51–64.
- Swail, V.R., Ceccacci, E.A., Cox, A.T., 2000. The AES40 North Atlantic wave reanalysis: validation and climate assessment. In: 6th International Workshop on Wave Hindcasting and forecasting, California, USA.
- Tedd, J., Kofoed, J.P., 2009. Measurements of overtopping flow time series on the Wave Dragon, wave energy converter. *Renew. Energy* 34 (3), 711–717.